THESIS

CONSERVATIVE SOLUTE TRANSPORT PROCESSES AND ASSOCIATED TRANSIENT STORAGE MECHANISMS: A COMPARISON OF STREAMS WITH CONTRASTING CHANNEL MORPHOLOGIES, LAND USE, AND LAND COVER

Submitted by

Karin Emanuelson

Department of Ecosystem Science and Sustainability

In partial fulfillment of the requirements

For the Degree of Master of Science

Colorado State University

Fort Collins, Colorado

Summer 2021

Master's Committee:

Advisor: Timothy Covino

Matthew R.V. Ross
Ryan R. Morrison

ABSTRACT

CONSERVATIVE SOLUTE TRANSPORT PROCESSES AND ASSOCIATED TRANSIENT STORAGE MECHANISMS: A COMPARISON OF STREAMS WITH CONTRASTING CHANNEL MORPHOLOGIES, LAND USE, AND LAND COVER

Land use within a watershed impacts stream channel morphology and hydrology and therefore in-stream solute transport processes. In this study, I selected two stream sites with contrasting channel morphology, land use and land cover: Como Creek, CO, a relatively undisturbed, high-gradient, forested stream with a gravel bed and complex channel morphology and Clear Creek, IA, an incised, low-gradient stream with low-permeability substrate draining an agricultural landscape. At these sites, I performed conservative stream tracer experiments to address the following questions: 1) How does solute transport vary between streams with differing morphologies and watershed land use?, and 2) How does solute transport at each stream site change as a function of discharge? I analyzed in-stream tracer time series data and compared results quantifying solute attenuation in surface and subsurface transient storage zones. I found significant differences in solute transport metrics between sites and significant trends in these metrics with varying discharge conditions at the forested site but not at the agricultural site. In the relatively undisturbed, forested stream there was a broad range of transport mechanisms and evidence of substantial exchange with both surface and hyporheic transient storage. In this forested site, changing discharge conditions activated or deactivated different solute transport mechanisms and greatly impacted advective travel time. Conversely, in a simplified, agricultural stream there was a narrow range of solute transport behavior across flows and predominantly surface transient storage at

all measured discharge conditions. These results demonstrate how channel simplification resulting from land use change inhibits available solute transport mechanisms across varying discharge conditions.

ACKNOWLEDGEMENTS

This thesis is a product of several years' of work and numerous people who have inspired and supported me during the pursuit of my Master's degree. In particular, I would like to thank my advisor, Tim Covino, for his overall guidance, support with field work, and generous time spent reviewing analysis and re-reading drafts. Additionally, I would like to thank my committee members, Matt Ross and Ryan Morrison, for teaching me valuable skills that have helped me meet my goals as well as always being supportive through the twists and turns of my path here at Colorado State University. I could not have completed this study without my field technicians, Andy Rohlf and Julia Young. You both kept me sane and smiling through long field days.

I would also like express thanks to my team members Joel Singley, Michael Gooseff, Kamini Singha, Jancoba Dorley, and Ricardo González-Pinzón. I greatly enjoyed working with you all and appreciated your support along the way. Each of you challenged me in different ways that ultimately developed both my education and this study. I would like to extend my deepest gratitude to my collaborator Adam Ward for getting in the weeds through the analysis and pointing me in the right direction to keep me moving forward.

Finally, I would not be here without the support of my friends, family and classmates. You all provide so much light and energy to my life that keeps me curious and motivated!

TABLE OF CONTENTS

1. INTRODUCTION

Diverse and widespread land use change has resulted in alteration of fluvial ecosystem across the United States (US). A recent report from the US Environmental Protection Agency (2020) classified 70% or 850,904 river and stream miles as impacted by at least one type of human influence (defined as: roads, pavement and cleared lots, buildings, pipes, parks or maintained lawns, trash, pastures and rangeland, row crops, dams, and logging or mining operations). These land cover changes can increase hydrologic connectivity between streams and the terrestrial landscapes they drain through tile drains and irrigation networks in agricultural systems (McIsaac and Hu, 2004; David *et al.*, 2009), impervious surfaces in urban environments (DeWalle *et al.*, 2000; Jones *et al.*, 2000). Conversely, levees (Kondolf *et al.*, 2006), mill-dams (Walter and Merritts, 2008), and river channelization (Pierce *et al.*, 2012) tend to decrease hydrologic connectivity within and along the river corridor.

Fluvial geomorphology and geomorphic complexity can enhance the exchange of water between the main channel and surrounding storage areas (e.g., pools, hyporheic zone), and consequently increase transient storage and solute residence times within a stream (Ensign and Doyle, 2005). Land-use change and water resource management can impact channel geomorphology through changes in water and sediment delivery (Magliozzi *et al.*, 2017), and therefore may impact stream solute transport processes. Given that many human alterations (e.g., channelization) of fluvial system lead to a reduction of geomorphic complexity (Covino, 2017), it follows that these anthropogenic alterations have the potential to decrease solute residence times. In fact, urban and agricultural land-use has been linked to decreased geomorphic complexity and significantly shorter transient storage residence times than relatively undisturbed reference systems (Gooseff *et al.*, 2007). Given the potential linkages between land use and solute transport, and the widespread land cover change in most of the US, it is important to understand how land use changes propagate into the stream channel, and how this may alter solute transport and the associated implications for downstream water quality (e.g., Brunke & Gonser, 1997; Krause et al., 2011; Ward, 2016; Wondzell & Gooseff, 2014).

Processes including advection, dispersion, and transient storage control how solutes are transported through a stream network and these processes occur in two major compartments: the advective flow and transient storage zones. Advective flow often comprises the majority of a stream or rivers cross-sectional area, where high velocities place important controls on median solute transport times (Johnson et al., 2014). Conversely, transient storage compartments have lower transport velocities and longer solute retention times relative to advective flow (Bencala and Walters, 1983; Harvey et al., 1996). Recent studies (Briggs *et al.*, 2009; Johnson *et al.*, 2014) have separated transient storage further into surface transient storage and hyporheic transient storage because these two compartments have different hydraulic and biogeochemical conditions (Runkel et al., 2003; Thomas et al., 2003).

Pools, eddies, and side channels contain dead zones and are the primary surface transient storage compartments. Water exchange into surface transient storage compartments is primarily controlled by dispersion (Fischer et al., 1979) and turbulent processes (Ghisalberti, 2002; Jackson *et al.*, 2015). Variation in discharge can activate or deactivate surface transient storage flow paths due to changes in turbulent energy, wetted geometry, and hydraulic gradients within the channel (Leopold and Maddock, 1953). Additionally, past studies have found that roughness elements (e.g., fallen logs, debris jams, shrubs, and grasses) can increase surface transient storage (Ader *et al.*, 2021).

Hyporheic transient storage compartments are located beneath and adjacent to the stream channel (Stanford and Ward, 1988) and are areas where water exchanges between the channel and the subsurface (Harvey *et al.*, 1996). Hydrostatically driven hyporheic exchange is primarily controlled by the local hydraulic gradient and bed conductivity (Boano *et al.*, 2014). Reach scale hydraulic gradients are driven by channel slope, width, and sinuosity (Sharp, 1977; Larkin and Sharp Jr., 1992) as well as temporal fluctuations in water table heights and channel stage (Pinder and Sauer, 1971). Past studies evaluating hyporheic transient storage at a reach-scale as a function of changing discharge conditions present conflicting findings. Morrice *et al.* (1997), Wondzell (2006), Fabian *et al.* (2011) show that hyporheic storage increases with increasing discharge, while Morrice *et al.* (1997), Butturini and Sabater (1999), Zarnetske *et al.* (2007), Schmid *et al.* (2010), Fabian *et al.* (2011) conclude hyporheic storage shrinks with increasing discharge. However, differences in timing and methods make intercomparison between these studies impossible. Additionally, superficial sediments located in the hyporheic zone significantly impact bed conductivity which in turn effects the rate of hyporheic exchange (e.g., presence of low conductivity streambed strata, Bencala *et al.*, 1984; Harvey and Wagner, 2000; Tonina and Buffington, 2009; Angermann *et al.*, 2012; Stonedahl *et al.*, 2013; Zimmer and Lautz, 2014).

In this study, I evaluated solute transport in two streams with contrasting channel morphology and land cover to address the following questions: 1) How does solute transport differ between a relatively undisturbed, high-gradient, forested stream with a gravel bed and complex channel morphology and a heavily impacted, low-gradient, channelized stream draining an agricultural landscape?; And 2) How does solute transport within each stream change as a function of discharge?

2. DATA AND METHODS

2.1 Site Descriptions

This research was conducted at two streams with contrasting land use, land cover, climate, and fluvial geomorphology. The forested stream in Colorado, USA is relatively undisturbed by human activities and has complex channel morphology. In contrast, the agricultural stream in Iowa, USA is highly modified system with limited geomorphic complexity.

The forested site study reach was a 500 m long portion of Como Creek, a tributary of Boulder Creek, with land cover consisting of approximately 20% alpine meadow/tundra and 80% conifer forest. The study reach drained a 5.4 km^2 catchment, with elevations ranging from 2900-3030 m, and mean average precipitation of 883 mm/y (Ries III *et al.*, 2017). The forested site had a snowmelt-driven hydrograph with discharges ranging from 1-980 L/s, and peak discharge typically occurring mid- to late-June (Figure 1C). The study reach was a multi-thread channel with substrate ranging from small gravel to bedrock underlain by glacial till (Natural Resources Conservation Service). Additionally, the channel had an average width to depth ratio of 11.5, sinuosity of 1.1, and average reach slope of 21% (Figure 1D).

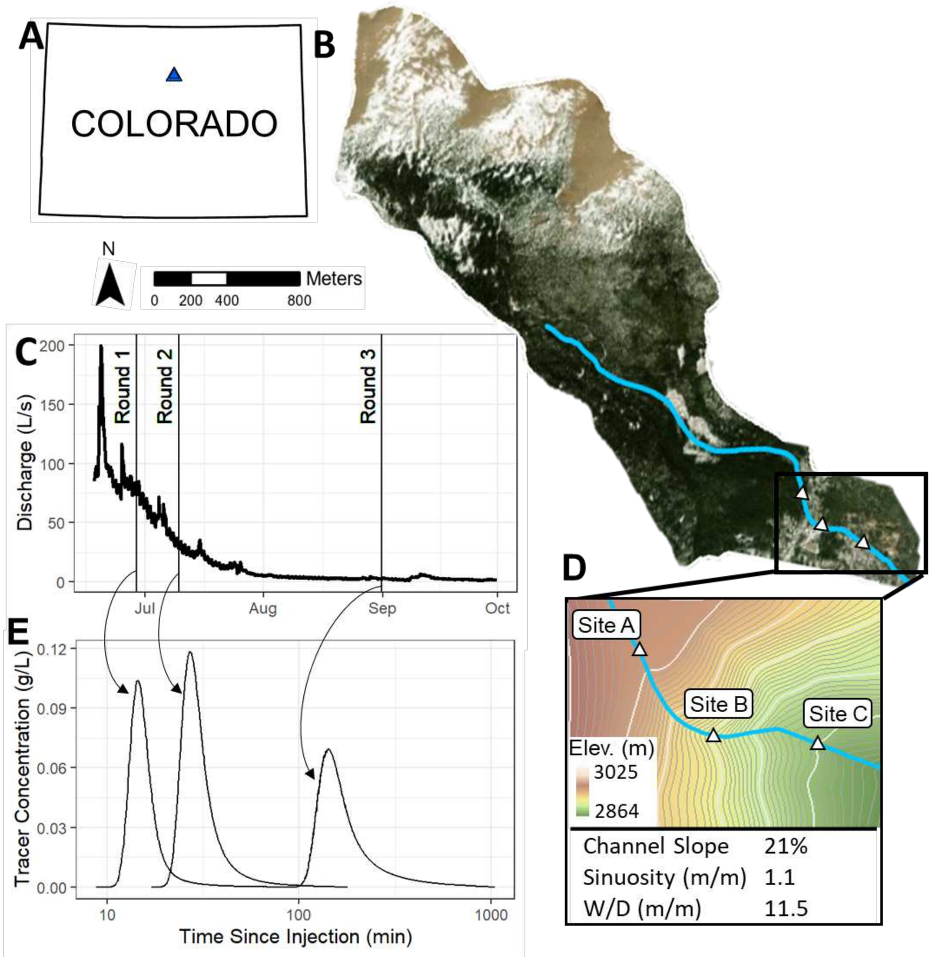

Figure 1: (a) Location of Como Creek Watershed in Colorado (Forested Site), (b) detailed map of Como Creek Watershed with satellite imagery showing land cover and locations of monitoring sites (white triangles), (c) hydrograph and timing of conservative tracer slug injections, (d) expanded study reach with monitoring sites, elevation contours, and reach information, and (e) example background corrected tracer breakthrough curves for each round from Reach A-B.

The agricultural reach was an 850 m portion of Clear Creek, a tributary of the Upper Mississippi River, with land cover consisting of approximately 93% cultivated crops and 6% urban land (Ries III *et al.*, 2017). It drained a 14.8 km^2 catchment, with elevations ranging from 197-248 m, and mean precipitation of 913 mm/y. The study reach was a single thread channel with a low gradient (0.8% slope), and width to depth ratio of 7.8 (Figure 2D). The channel was straightened to a sinuosity of 1, incised approximately 3.5 m and underlain by a silty clay loam substrate (Natural Resources

Conservation Service). These channel modifications and an extensive network of tile drains resulted in a flashy hydrograph with discharge varying from 70-15,000 L/s (Figure 1D).

To characterize the composition of substrate material smaller than 8 mm, I took 10 sediment samples along each study reach, created a composite sample and conducted a sieve analysis. At the forest site I found 64.3% gravel, 34.9% sand and 0.5% fines. Additionally, I observed a substantial amount of substrate (i.e. large gravel, cobbles, and boulders) larger than 8 mm that was not included in the analysis. Alternatively at the agricultural site, I did not observe any substrate greater than 8 mm and the composition of the substrate was 18.6% gravel, 50.5% sand and 31.0% fines.

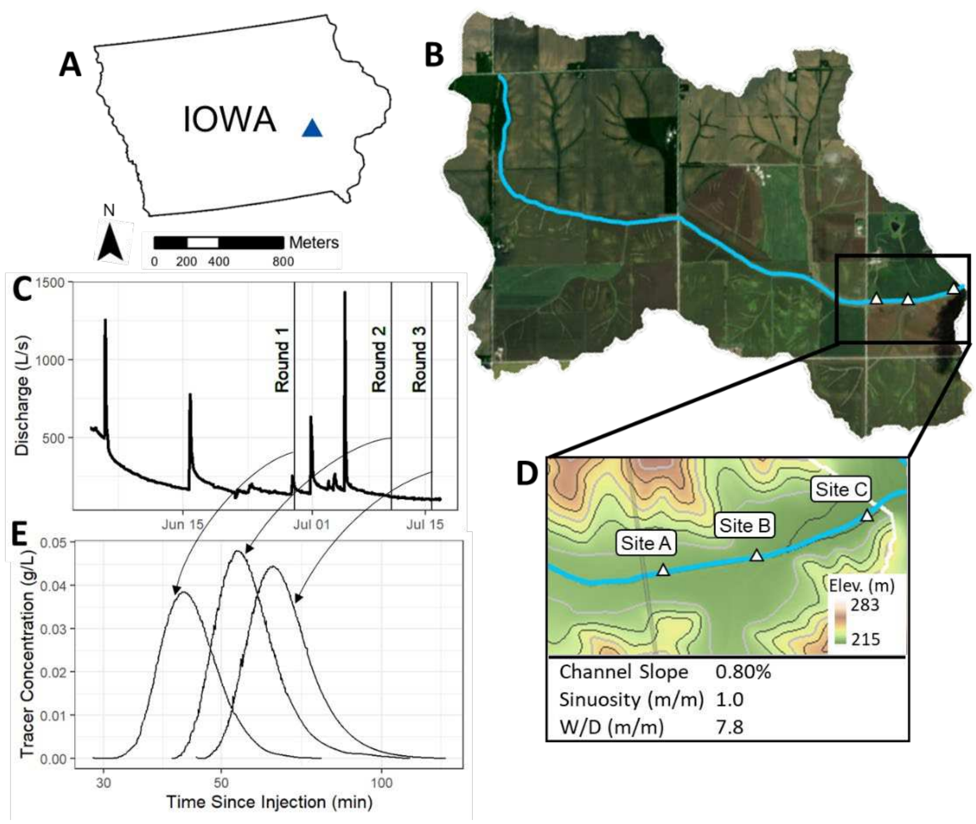

Figure 2: (a) Location of Clear Creek Watershed in Iowa (Agricultural Site), (b) detailed map of Clear Creek Watershed with satellite imagery showing land cover and locations of monitoring sites, (c) hydrograph and timing of conservative tracer slug injections, (d) subset of Clear Creek showing study reach with monitoring sites and elevation contours showing channel gradient (0.8% slope), and (e) example background corrected tracer breakthrough curves for each round from Reach A-B.

2.2 Field Methods

At both the forested and agricultural sites, I completed the same field experiments and collected analogous data. Field experiments at the agricultural site occurred on June 29th, July 11th, and July 16th 2019 with discharges of 155, 117, and 104 L/s respectively (Table 1). At the forested site, experiments occurred on June 29th, July 10th, and August 31st 2020 with discharges of 77, 28, and 3 L/s respectively (Table 1).

Table 1: Summary of reach characteristics, percent change in net discharge (*Qnet%*) and percent gross hydrologic loss (*% Gross Loss*). For *Qnet%* and *% Gross Loss* I show both the calculated values and error bounds. Error bounds were developed assuming a typical 10% error for dilution gauging (Schmadel *et al.*, 2010), and bold text indicates that the *Qnet%* or *% Gross Loss* is more positive than +10% or more negative than -10% (i.e., zero *Qnet%* or *% Gross Loss* is not included within the error bounds).

Stream Site	Round	Date	Reach Avg Q (L/s)	Stream Reach	Distance (m)	Advective Travel Time (min)	Qnet%		% Gross Loss	
							value	Error bounds	value	Error bounds
Agricultural	1	6/29/19	155	A-B	434	42.3	**14.5**	**(4.5 - 24.5)**	-7.3	(-17.3 - 2.7)
Agricultural	1	6/29/19	155	B-C	587	56.6	2.8	(-7.2 - 12.8)	-5.5	(-15.5 - 4.5)
Agricultural	2	7/11/19	117	A-B	434	53.3	**15.8**	**(5.8 - 25.8)**	0.0	(-10.0 - 10.0)
Agricultural	2	7/11/19	117	B-C	587	70.3	2.9	(-7.1 - 12.9)	-4.6	(-14.6 - 5.4)
Agricultural	3	7/16/19	104	A-B	434	62.4	**28.3**	**(18.3 - 38.3)**	0.0	(-10.0 - 10.0)
Agricultural	3	7/16/19	104	B-C	587	81.3	**30.9**	**(20.8 - 40.8)**	0.0	(-10.0 - 10.0)
Forested	1	6/29/20	77	A-B	263	13.9	3.9	(-6.1 - 13.9)	0.0	(-10.0 - 10.0)
Forested	1	6/29/20	77	B-C	282	15.6	-6.0	(-16.0 - 4.0)	-4.0	(-14.0 - 6.0)
Forested	2	7/10/20	28	A-B	263	27.1	-5.9	(-15.9 - 4.1)	0.0	(-10.0 - 10.0)
Forested	2	7/10/20	28	B-C	282	30.8	-4.2	(-14.2 - 5.8)	**-13.9**	**(-23.9 - (-3.9))**
Forested	3	8/31/20	3	A-B	263	142.2	**-19.1**	**(-29.1 - (-9.1))**	**-26.4**	**(-36.4 - (-16.4))**
Forested	3	8/31/20	3	B-C	282	232.3	-8.8	(-18.8 - 1.2)	**-74.7**	**(-84.7 - (-64.7))**

At each stream site, I established three continuous monitoring stations at the upstream, middle and downstream locations (Site A, B, and C, Figure 1D and 2D) where I recorded stream specific conductivity (SC) and temperature at 5-second intervals, as well as stream stage at 10-minute intervals. The instrumentation at these monitoring stations included SC and temperature sensors (Campbell Scientific CS547A) installed at mid-depth in the thalweg and pressure transducers (Campbell Scientific CS420) to measure stage installed in stilling wells. These sensors (SC and stage) were connected to Campbell Scientific CR 1000 dataloggers, which recorded and stored all data.

In addition to the field experiments, I constructed a stage-discharge relationship at the most downstream monitoring station (Site C) at each field site. This relationship was constructed through a series of NaCl dilution gauging injections and associated stage measurements throughout the field season to capture the full spectrum of discharge conditions. I used this relationship to create a continuous (10-minute) timeseries of discharge from the stage measurements throughout the field season (Figure 1C and 2C).

2.2.1 Dilution Gauging Injections

For the field experiments' dilution gauging injections, I mixed the conservative tracer with stream water and instantaneously injected this mixture into the channel approximately one mixing length upstream (84-88 m at agricultural site and 13-55 m at forested site) of each monitoring station to ensure complete mixing and negligible tracer loss. I began at the most downstream monitoring station (Site C) then moved upstream (Site B then Site A) allowing enough time for the preceding slugs to completely pass the downstream station before beginning the next injection. I recorded the specific conductivity BTCs at each monitoring station prior to tracer arrival, through the BTC and after the stream returned to background conditions. Then, I converted background-corrected specific conductivity to NaCl concentration using a conversion factor of 0.5 based on the molar mass and molar ionic conductivity of sodium chloride ions (Gibson, 2018). I analyzed tracer data to determine the net changes in discharge (as described below) to determine whether each stream was gaining or losing.

2.2.2 Reach-Scale Injections

For the reach-scale injections, I conducted a series of two conservative tracer (NaCl) slug injections at three different discharge conditions (six injections total). For each reach, I injected tracer instantaneously at the upstream monitoring station (Site A or B) and measured SC BTCs at the most downstream monitoring station (Site B or C). I again moved from downstream (Reach B-C) to upstream (Reach A-B) ensuring that the preceding slugs completely passed through the reach (i.e., to return to background conditions) before beginning the next injection. I varied stream reach lengths (434-587 m at the agricultural site and 263-282 m at the forested site, Table 1) in order to obtain similar solute travel times between the stream sites. Advective solute travel time was calculated as the time from injection to the peak of the BTC (t_{peak}). I adjusted reach lengths to obtain similar advective travel times between sites to enable cross-site comparison. Then, I converted background-corrected specific conductivity to concentration NaCl using the same conversion factor as discussed above. Example background corrected tracer BTCs at each site for the three different discharge conditions measured are presented in Figure 1E and 2E. I used this reach-scale injection tracer data to evaluate gross hydrologic loss, temporal metrics and StorAge Selection (SAS) functions (as described in the following selections). Gross hydrologic loss provides information on tracer and water lost to longer flowpaths with residence times from hours to days. Whereas, temporal moments and SAS functions give us information on shorter flowpath exchanges (residence times from minutes to hours) between the advective main channel and transient storage zones.

2.3. Net Changes in Discharge

First, I calculated discharge, Q, via dilution gauging (Kilpatrick and Cobb, 1985) from mixing length-scale tracer injections as

$$Q = \frac{M}{\int_{\tau=0}^{\tau=t} C(\tau)d\tau} \tag{1}$$

Where M is the tracer mass added to the stream, C is the background corrected NaCl concentration and t is the time between injection (τ =0) and return to background (τ =t). I then determined the net change in discharge ($\Delta Qnet$) across the stream reaches as

$$\Delta Qnet = Q_D - Q_U \tag{2}$$

Where Q_D is the discharge at the downstream monitoring site and Q_U is the discharge at the upstream monitoring site. I converted this to $Qnet\%$ by dividing by Q_U.

$$Qnet\% = \frac{\Delta Qnet}{Q_U} * 100 \tag{3}$$

Positive values of *Qnet%* indicate a net gaining reach whereas negative values a net losing reach. Dilution gauging is subject to several sources of error (Zellweger *et al.*, 1989). Tracer was released one mixing length above the monitoring station yet, if some mass was lost over this section, discharge will be overestimated. Therefore, I applied error bounds to *Q* and *Qnet%* assuming a 10% error for dilution gauging (Schmadel *et al.*, 2010).

2.4 Gross Hydrologic Loss

Using the discharge estimates determined above combined with the reach-scale tracer BTCs, I calculated tracer mass recovery (M_R) as

$$M_R = Q_D \int_{\tau = t_1}^{\tau = t_{99}} C_{UD}(\tau) d\tau \tag{4}$$

where C_{UD} is the background corrected conservative tracer (NaCl) BTC concentration at the downstream monitoring site from upstream conservative tracer release and *t* is the time between the first tracer arrival at the downstream site ($\tau = t_1$) and the time at which 99% of the BTC passes by the monitoring station ($\tau = t_{99}$). t_{99} was used as the upper limit to reduce the subjective selection of an end of the observed tracer BTC and to alleviate issues with sensitivity that occur at late BTC waiting times (after Drummond *et al.*, 2012; Mason *et al.*, 2012; Ward *et al.*, 2013c, 2013b; Schmadel *et al.*, 2016).

Next, I determined tracer mass loss (M_L) throughout each reach as, $M_L = M_R - M_U$, and percent gross loss as

$$\%\ Gross\ Loss = \frac{M_L}{M_U} * 100 \tag{5}$$

where M_U is the tracer mass injected at the upstream monitoring site. For cases where a positive gross loss was calculated in a net gaining reach, I assumed that no mass was lost (M_L=0). Possible interpretations for gross loss within a system include the tracer labeled water was retained in storage beyond the timescale of the experiment, exchanged with water that was not labeled with tracer or entered a subsurface storage compartment and was returned to streamflow downstream of the monitoring station (Payn *et al.*, 2009). Because gross loss relies on discharge estimates derived from dilution gauging, I additionally applied the 10% error associated with dilution gauging to gross loss estimates and only considered gross loss to be non-zero if it was greater than 10%.

2.5 Temporal Metrics

The shape of a BTC provides a reach-average representation of interactions between advection, dispersion and transient storage (Schmadel *et al.*, 2016). Using the observed BTC of the reach-scale tracer injections, I first calculated the transient storage index, *TSI*. *TSI* is the time elapsed between the advective time (time of BTC peak, t_{peak}) and the time at which 99% of the in-channel BTC passed by the monitoring station (t_{99}). *TSI* provides an indicator of transient storage (information in tail) relative to advective transport (information in peak).

$$TSI = t_{99} - t_{peak} \tag{6}$$

Additionally, I normalized NaCl concentrations (*c(t)*) to express only the available temporal signature as

$$c(t) = \frac{C(t)}{\int_{t=t_1}^{t=t_{99}} C(t)dt}. \tag{7}$$

where *C(t)* is the background corrected NaCl concentration and *t* is time since injection. Next, I calculated temporal moments of the tracer BTCs to quantify advective transport, spreading, and tailing behaviors. The first temporal moment (M_1), which represents the mean travel time through the study reach, was calculated as

$$M_1 = \int_{t=0}^{t=t_{99}} tc(t)dt. \tag{8}$$

Next, I calculated higher-order central moments (μ_n), or moments taken about mean arrival time (M_1).

$$\mu_n = \int_{t=0}^{t=t_{99}} c(t)(t - M_1)^n dt \tag{9}$$

The second central temporal moment (μ_2), is the variance of the tracer time series. It provides a measure of symmetrical spreading of the breakthrough curve from mean arrival time (M_1). The third central temporal moment (μ_3) provides a description of asymmetry typically attributed to late-time tailing (Gupta and Cvetkovic, 2000).

From these temporal moment metrics, I calculated the coefficient of variation (*CV*) and skewness (γ). The coefficient of variation and skewness (*CV* and γ) are preferable to the second and third central moments (μ_2 and μ_3) because they reflect normalization by advective time and variance, respectively (Ward *et al.*, 2018). This normalization helps distinguish differences that arise because of experimental limitations from those associated with changes in dispersive and short-term storage processes.

The coefficient of variation (*CV*) is calculated as

$$CV = \frac{\mu_2^{1/2}}{M_1}. \tag{10}$$

CV represents the rate of symmetrical spreading relative to mean arrival time. High *CV* values indicate increased importance of non-advective processes (e.g., dispersion and transient storage) on reach solute transport. Skewness (γ) of the BTC is calculated as

$$\gamma = \frac{\mu_3}{\mu_2^{3/2}}. \tag{11}$$

γ reflects the extent of late-time tailing relative to symmetrical spreading. High γ values indicate non-symmetrical tracer BTCs with long tails, whereas low γ values indicate more symmetrical BTCs similar to a normal distribution.

Finally, I calculated holdback (*H*) of the system, which describes transport in the system ranging from pure advection (where *H*=0) to only dispersive transport (*H*=1) (Danckwerts, 1953) and is calculated as

$$H = \frac{1}{M_1} \int_{t=0}^{t=M_1} F(t)dt \tag{12}$$

where,

$$F(t) = \int_{\tau=0}^{\tau=t} c(\tau)d\tau. \tag{13}$$

2.6 StorAge Selection (SAS) Analysis

I analyzed the reach-scale tracer data following the StorAge Selection (SAS) function approach described by Ward *et al.* (2019b) and adapted from Harman *et al*. (2016). The SAS approach provides information on the age of water exiting a study reach. The age is determined by the residence times of different storage compartments experienced by each water parcel and is related to transit time distributions (TTDs, the probability density function of a water parcel's age when it exits a control volume). However, this SAS approach differs from TTDs by isolating the contribution of storage turnover to the transit time from that of inflow and outflow variability (Ward *et al.*, 2019b). This method assumes discharge was at steady state during each injection and thus sets the forward (inflow) and backward (outflow) TTDs equal. With this assumption, I can directly calculate the probability density function and the cumulative form of the (forward) TTD to gain an understanding of the volume of stream water that is actively turning over during the field experiment.

First, I calculated the probability density function of the transit time distribution ($p_Q(T)$) as,

$$p_Q(T) = \frac{QC_{obs}(T)}{M_U} \tag{14}$$

where T is defined as the age of a parcel of water in seconds where at the time of injection the water is assigned an age of zero (T=0). Plainly, this describes the probability that a parcel of water exiting the reach has an age T. I then calculated the cumulative form of the transit time distribution ($P_Q(T)$) as,

$$P_Q(T) = \int_{\tau=0}^{\tau=T} p_Q(\tau)d\tau \tag{15}$$

where, τ is a random variable ranging from the time of injection (τ =0) to the oldest age observed by the tracer (τ =T). This can be interpreted as the distribution of ages of water exiting the reach that were labeled by the tracer. From this, I determine the age-ranked discharge ($Q_T(T)$) or the rate that water equal to or younger than some age, T, is leaving the reach as

$$Q_T(T) = QP_Q(T). \tag{16}$$

Errors in discharge can cause physically impossible $Q_T(T)$ values. Therefore, I assumed a typical error of 10% for dilution gauging (Schmadel *et al.*, 2010), calculated the range of physically plausible discharges and analyzed the midpoint of the plausible range in order to get physically meaningful SAS calculations (after Harman *et al.*, 2016; Ward *et al.*, 2019a). I calculated the cumulative age-ranked storage ($S_T(T)$) as

$$S_T(T) = Q\left(T - \int_{\tau=0}^{\tau=T} P_Q(\tau)\, d\tau\right). \tag{17}$$

The age-ranked storage is a measure of the volume of water stored in the reach that is younger than some age T. In my case, the minimum value, $S_{T,min}$, is the pure advection volume of the reach (i.e., youngest age the water can have after traveling from the injection point to the monitoring location which occurs after one volume of stream water is discharged from the system, or plug flow). The maximum value, $S_{T.max}$, is the maximum volume of storage that is actively turning over on timescales that the tracer labeled water can exchange with. This is equal to only a fraction of the total storage available in the reach due to limitations arising from the window of detection (i.e., the known limitation that solute tracers cannot access storage beyond the timescale at which tracer cannot be differentiated from background conditions; Harvey *et al.*, 1996).

Additionally, I computed the complement of the age-ranked discharge which describes the rate of water leaving the reach that is older than some age T, respectively as,

$$Q_{comp} = Q\left(1 - P_Q(T)\right). \tag{18}$$

I interpret the minimum value of the age-ranked discharge complement ($Q_{comp,min}$) as the rate of water leaving the stream reach that was not labeled by the tracer within the timescale of the experiment. Plausible explanations for unlabeled discharge include water that enters the reach through subsurface flowpaths (i.e., lateral inflow of unlabeled water), water that was labeled with tracer upstream but follows a subsurface flowpath that returns to the stream downstream of the reach (missing detection by the downstream sensor) and water that was labeled with tracer yet remains in storage beyond the timescale of the tracer experiment (Payn *et al.*, 2009).

Because both discharge and volume sampled are dependent on reach lengths, I calculated normalized reference values to compare between reaches and stream sites. First, I determined the fraction of the total in-stream discharge that was labeled with the tracer ($f_{Q,label}$) as,

$$f_{Q,label}(T) = \frac{Q_{comp,max} - Q_{comp,min}}{Q} \tag{19}$$

Past studies (Ward *et al.*, 2019b) calculated $f_{Q,label}$ as the fraction of the total down-valley discharge (both in-stream and subsurface discharge). Due to the lack of subsurface data available at the stream site, I could not quantify subsurface discharge and therefore calculated this fraction only in respect to in-stream discharge. This reference value ranges from 0 to 1 where high values of $f_{Q,label}$ indicate that most of the water exiting the reach was labeled with tracer or tracer labeled water experienced shorter flowpaths with residence time lesser or equal to the experimental timescale. Alternatively, low $f_{Q,label}$ values indicate labeled water was retained the system longer than the timescale of the experiment.

Finally, I calculated the fraction of the advective volume sampled (f_{VADV}) as,

$$f_{VADV}(T) = \frac{S_{T,max}}{V_{adv}} \tag{20}$$

where $S_{T.max}$, is the maximum volume of storage that is actively turning over on timescales that the tracer labeled water can exchange with and V_{adv} is the volume of the stream water in advection (discharge*advective time). f_{VADV} values equal to 1 indicate that tracer labeled water only experienced advective flow. I interpret f_{VADV} values slightly greater than 1 to indicate that tracer labeled water experienced storage in surface transient storage and f_{VADV} values much greater than 1 to indicate tracer labeled water experienced storage in both surface transient storage and hyporheic transient storage. A summary of all the variables used in this study is available in Appendix A.

2.7 Statistical Tests

2.7.1 Differences between Study Sites

To quantify differences in solute transport metrics between the agricultural and forested site, I completed a nonparametric test to compare medians using a Kruskal-Wallis one-way ANOVA on ranks (resulting p-values reported as p_{KW}). While this test is similar to comparing means with the one-way analysis of variance (ANOVA), I chose this nonparametric method because it does not assume a normal distribution of the residuals and prevents over interpreting results from the small sample size. Additionally, I evaluated the homogeneity of variance between the two sites with the Brown-Forsythe test, based on deviations from group medians (resulting p-values reported as p_{BF}). This test was chosen because it is less sensitive to departures from normality which again prevents over interpreting results from small sample sizes. Results of these tests were considered significant if the p-value was less than 0.05.

2.7.2 Relationships with Advective Time

To quantify how solute transport varied with changing discharge conditions, I evaluated relationships between advective solute travel time and solute transport metrics for each stream site (forested and agricultural). As described in section 2.2.2 Reach-scale injections, I selected reach lengths at each stream site to enable comparable advective timescales and allow for cross-site comparison. For a given reach length, advective time becomes longer as discharge decreases and shortens as discharge increases. To develop confidence in the test results despite the small sample size, I bootstrapped the data with 100 replicates and evaluated the 95% confidence interval of the resulting slopes. I determined that a slope was significant if the 95% confidence interval did not include a slope of zero. Only the confidence interval and direction of significant slopes are reported to avoid over interpreting results.

3. RESULTS

3.1 Net Changes in Discharge

There were significantly different percent net changes in discharge (*Qnet%*) when comparing between the agricultural and forested streams (p_{KW}=1.04E-02, Table 2). The agricultural site was generally a net gaining reach whereas the forested site was primarily net neutral (Figure 3A). All *Qnet%* values reported in this section are the absolute value but have an associated ±10% error (Table 1; Figure 3). At the agricultural site, the *Qnet%* ranged from 3 to 31 %. I observed net gains greater than 10% during all injection rounds in reach A-B, but only at the longest advective time (i.e., lowest discharge) in reach B-C (Table 1). In the forested site, *Qnet%* ranged from -19.1% to 3.9% but I only observed a net change beyond the bounds of error (-19.1%) in reach A-B during injection round 3 (Table 1). I did not observe significant slopes (i.e., confidence interval of the slope did not include zero) in the relationships between *Qnet%* and advective time at either the agricultural or forested sites (Figure 3 and Table 2).

Table 2: Summary of statistical analysis. Bold font and * and ** indicates significant p-value at p < 0.05 and p < 0.01 respectively. I used Brown-Forstythe (p_{BF}) to test the difference in variance between data at the Agricultural and Forested sites and Kruskal-Wallis (p_{KW}) to test the difference in median values between sites. For trends of each metric with advective time, the upper and lower 95% confidence interval of the slopes is provided. The direction of the trend is indicated as increasing "+" or decreasing "(-)". NA indicates the trend between metric and advective travel time was not significantly different than zero.

	Difference in Variance			Difference in Medians			Trend with Advective Travel Time					
	Agricultural	Forested	p_{BF}-value	Agricultural	Forested	p_{KW}-value	Agricultural			Forested		
	range	*range*		*median*	*median*		*lower CI*	*upper CI*	*trend*	*lower CI*	*upper CI*	*trend*
Qnet%	2.8 - 30.9	-19.1 - 3.9	2.31E-01	**15.2**	**-5.9**	**1.04E-02***	-0.838	1.71	NA	-0.228	0.0993	NA
% Gross loss	-7.3 - 0	-74.7 - 0	1.27E-01	-2.3	-8.9	3.19E-01	-0.214	0.335	NA	**-0.635**	**-0.187**	**(-)***
Transient Storage Index (TSI)	18.1 - 42.2	38.9 - 661	1.18E-01	**33.7**	**72.9**	**1.63E-02***	-0.157	1.01	NA	**1.6**	**5.13**	**+***

Mean Arrival Time (M_1)	44.7 - 84.5	16.7 - 347	1.73E-01	62.3	35	3.37E-01	**0.832**	**1.14**	**+***	**1.19**	**1.58**	**+***
Holdback (H)	0.41 - 0.53	0.39 - 0.6	5.40E-01	0.48	0.51	5.22E-01	-0.0058	0.00127	NA	**-0.00584**	**-0.00055**	**(-)***
Skewness (γ)	0.59 - 1.32	1.48 - 3.42	1.80E-01	**1.15**	**2.37**	**3.95E-03****	0.00338	0.0287	NA	-0.0477	0.00138	NA
Coefficient of Variation (CV)	0.11 - 0.15	0.31 - 0.58	5.37E-02	**0.13**	**0.38**	**3.95E-03****	-0.001	0.00152	NA	-0.00059	0.0023	NA
Advective Travel Time (t_{peak})	42.3 - 81.3	13.9 - 232	1.91E-01	59.5	28.9	3.37E-01						
Fraction of Q labeled (f_{Qlabel})	0.93 - 0.97	0.51 - 0.97	1.08E-01	0.94	0.91	4.23E-01	-0.0011	0.00137	NA	**-0.00311**	**-0.0012**	**(-)***
Fraction of Advective Vol (f_{VADV})	1.07 - 1.17	1.24 - 3.14	1.07E-01	**1.11**	**1.53**	**3.95E-03****	-0.0046	0.00098	NA	-0.00052	0.0148	NA

3.2 Gross Hydrologic Loss

Similar to values of net changes in discharge, all gross loss values reported in this section are reported as the absolute value but have an associated ±10% error (Table 1 and Figure 3). Additionally, due to this error I only consider gross losses as non-zero when they are greater than -10%. While the variance and median values of percent gross loss were not significantly different between sites (p_{KW}=3.19E-01, p_{BF}=1.27E-01, Table 2), I observed different gross loss dynamics between sites. At the agricultural site, no substantial gross loss was seen, and values ranged from 0 to -7.3% (Table 2). In contrast, at the forested site, substantial gross loss was observed during round 2 at reach B-C (-13.9%) as well as during round 3 at both reach A-B and B-C (-26.4% and -74.7%, respectively, Table 1). I observed a statistically significant decreasing slope with more gross loss at longer advective times (i.e., lower discharge conditions) at the forested site (CI = [-0.635 – (-0.187)]), but no relationship at the agricultural site (Table 2, Figure 3B).

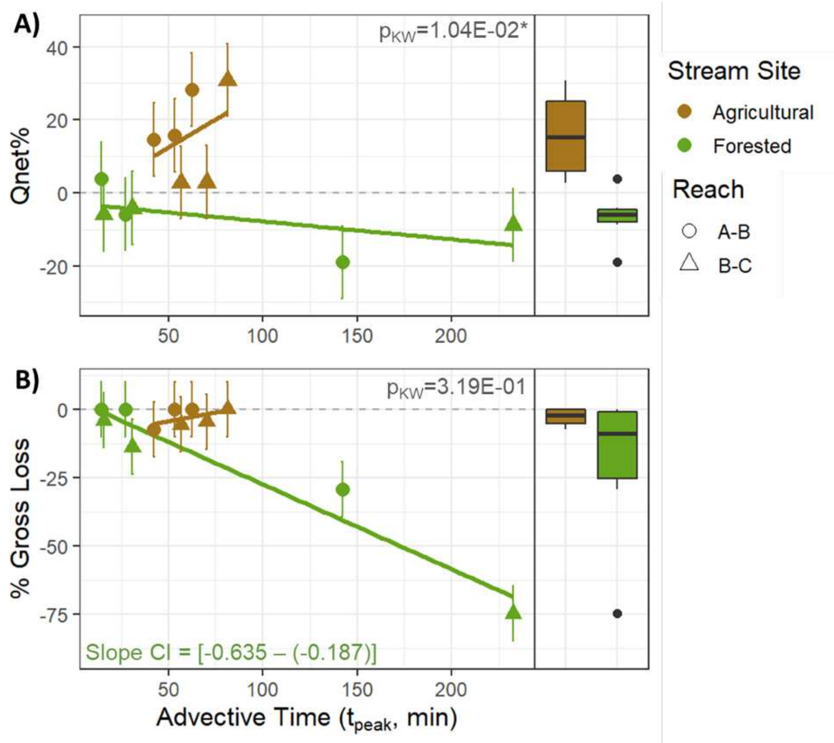

Figure 3: Summary of channel water balance metrics, net change in discharge (% Net Δ Q) and % mass loss. Error bars on scatterplots indicate ± 10%. I only consider Qnet or Gross Loss to be non-zero if error bars do not cross zero (indicated by the gray dashed line). The confidence interval of the slope (Slope CI) in the corresponding stream site color is shown in the lower left-hand corner only if slope is significant. Boxplots show variance and median value at each stream. The results (p_{KW}) of the Kruskal-Wallis test comparing medians values are shown to the left of boxplots, with 95% and 99% significant difference in medians indicated as * and ** respectively.

3.3 Temporal Metrics

In the study design, I aimed to achieve comparable magnitudes of advective solute travel times in both the forested and agricultural sites. While I was able to capture similar magnitudes of advective times in both the agricultural and forested sites, the overall variance in advective time was narrower in the agricultural site (Figure 4F & Table 2). Specifically, at the forested site I observed a broad range in advective time (14 – 232 min) relative to the agricultural site (42 – 81 min).

I observed that median values of transient storage index (*TSI*), skewness (γ) and coefficient of variation (*CV*), were significantly different between sites (Table 2, Figure 4A, D, &E). *CV* measures symmetrical spreading relative to mean arrival time. I interpret higher values of *CV* observed at the forested site to indicate that there is more dispersion and transient storage within these reaches compared to the agricultural site. Additionally, *TSI* and γ quantify the extent of late time tailing. Higher values of *TSI* and γ both indicate transient storage is more pronounced at the forested site than the agricultural site.

While I observed a wider range of values in *TSI* and mean arrival time at the forested site compared to the agricultural site (Figure 4), the variance of values for all temporal moment metrics were not statistically significantly different between stream sites (Table 2). At the agricultural site, I observed a narrow range in *TSI* (18.1-42.2 mins) and mean arrival time values (44.7 –84.5 mins), in contrast to the broad range at the forested site for both *TSI* (38.9 – 661 mins) and mean arrival time values (16.7 – 347 mins) (Table 2, Figure 4A&B).

I observed a significant, positive trend between mean arrival time and advective time at both the agricultural and forested sites (Figure 4B). However, none of the other relationships between temporal moment metrics and advective time were significant at the agricultural site (Figure 4). Conversely, at the forested site, *TSI*, mean arrival time, and holdback (*H*) all showed significant relationships with advective time (Figure 4, Table 2). At longer advective timescales (i.e., lower discharge conditions) solutes move more slowly resulting in higher mean arrival times at both stream sites (Figure 4B). At the forested site, I observed an increase in *TSI* at longer advective times (Figure 4A). I interpret an increase in *TSI* to demonstrate that the forested site has longer tailing behavior and more transient storage available at longer advective times. Holdback values were negatively related to advective times in the forested reaches, which represents less retention of injected tracer at longer advective times (Figure 4C).

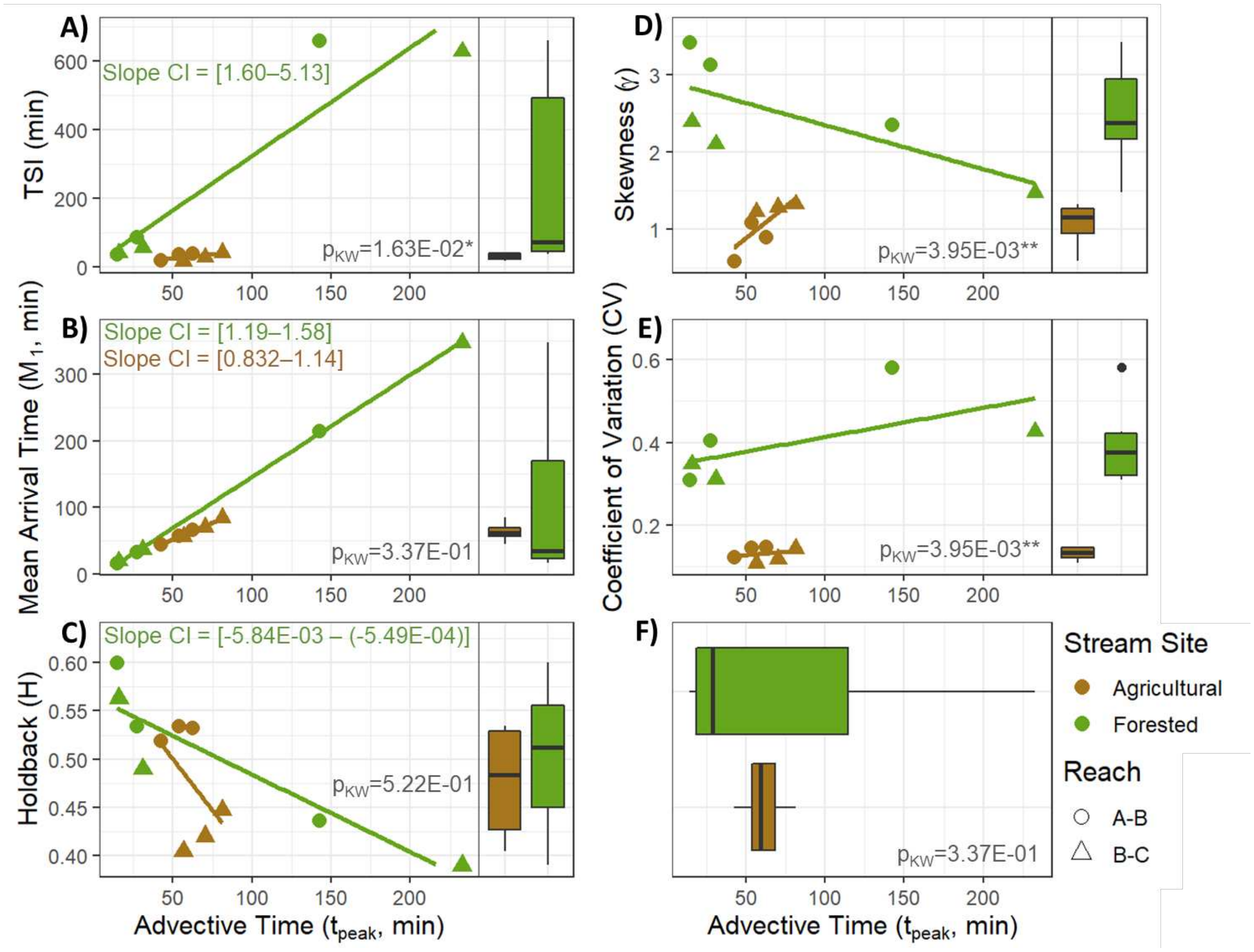

Figure 4: Summary of temporal moment analysis metrics, Transient Storage Index (TSI), mean arrival time (M_1), Holdback (H), Skewness (γ), Coefficient of Variation (CV), and Advective Time (t_{peak}). The confidence interval of the slope (Slope CI) in the corresponding stream site color is shown in the upper left-hand corner only if slope is significant. Boxplots show variance and median value at each stream. The results (p_{KW}) of the Kruskal-Wallis test comparing medians are shown to the left of boxplots, with 95% and 99% significant difference in medians indicated as * and ** respectively.

3.4 StorAge Selection (SAS) Analysis

I observed similar median values of f_{Qlabel} (p_{KW}=4.23E-01, Table 2, Figure 5A) between the agricultural and forested sites. Conversely, the forested site had significantly higher median values of f_{VADV} (p_{KW}=3.95E-03, Table, Figure 5B). f_{VADV} measures the fraction of the advective volume sampled where values slightly greater than 1 indicate that tracer labeled water experienced storage likely in surface transient storage and f_{VADV} values much greater than 1 indicate tracer labeled water most probably experienced storage in both surface transient storage and hyporheic transient storage. Values of f_{VADV} for the forested site were always greater than the agricultural site indicating that tracer labeled water in the forested site experienced longer flowpaths and exchanged with both surface and hyporheic transient storage. This is consistent with patterns in f_{Qlabel} where low values indicate solute loss to flowpaths with longer residence times and high values indicate solute remained within flowpaths with short residence times likely in surface transient storage. I observed a broader range of f_{Qlabel} values at the forested site (0.51 – 0.97, Table 2) indicating tracer labeled water experienced flowpaths with both short and long residence times associated with surface and hyporheic transient storage respectively. In contrast at the agricultural site, I observed low f_{VADV} values (1.07 – 1.17, Table 2) close to 1 and consistently high f_{Qlabel} values (0.93 – 0.97, Table 2, Figure 5). Taken together the results from the agricultural site suggest that tracer consistently only experienced surface transient storage and that there is little to no exchange between the stream and the hyporheic zone at the agricultural site.

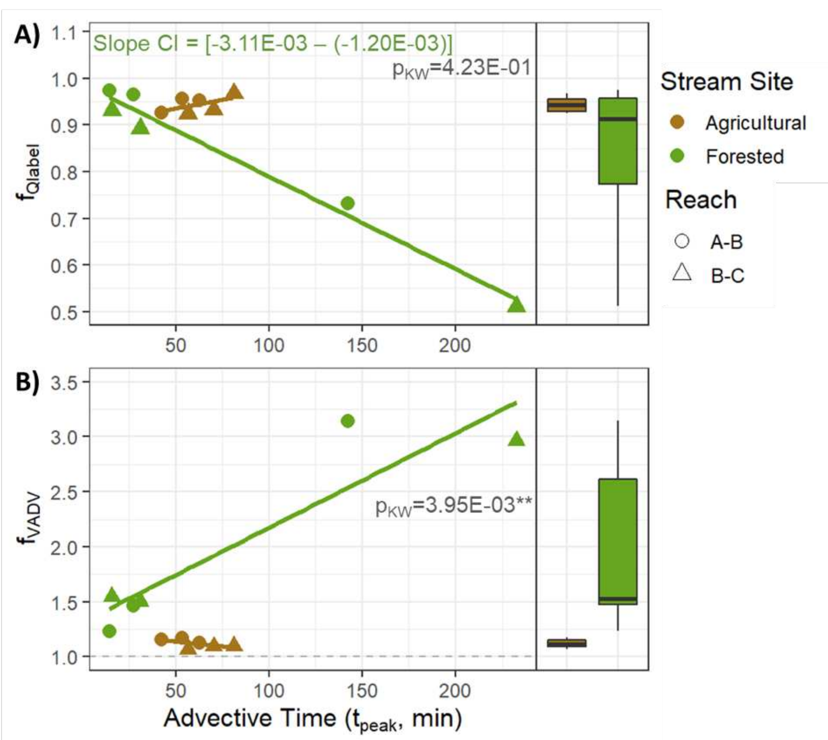

Figure 5: Summary of storage selection function metrics, fraction of discharge labeled (f_{Qlabel}) and fraction of advective volume labeled (f_{VADV}). The gray dashed line shown on the f_{VADV} plot is the lower bound of this reference value and indicates that tracer labeled water only experienced advective flow.

f_{VADV} values further above this line indicate tracer labeled water experienced more transient storage than f_{VADV} values close to the lower bound. The confidence interval of the slope (Slope CI) in the corresponding stream site color is shown in the upper left-hand corner only if slope is considered significant. Boxplots show variance and median value at each stream. The results (p_{KW}) of the Kruskal-Wallis test comparing medians are shown to the left of boxplots, with 95% and 99% significant difference in medians indicated as * and ** respectively.

I observed a decrease in f_{Qlabel} as advective time increased at the forested site but no trend between these metrics at the agricultural site (Table 2, Figure 5A). This indicates that at longer advective times or lower discharge conditions tracer labeled water in the forested stream was more likely to experience subsurface storage or be retained in storage for longer than the timescale of the experiment. In contrast to f_{Qlabel}, I did not observe a statistically significant relationship at either site between f_{VADV} and advective times (Table 2, Figure 5B). At the agricultural site, the lack of relationship for both f_{Qlabel} and f_{VADV}, with advective time (Table 2) combined with the narrow range of values for these metrics, suggests that the tracer labeled water exchanged with similar in-channel storage zones at various discharge conditions.

This SAS approach assumes steady state discharge during each injection. In the experiments, discharge was relatively constant (change of 10% or less) during the majority of the tracer injections, yet this assumption was not always met. Discharge changed more than 10% at the agricultural site during round 2 in both reach A-B (23%) and B-C (21%), and round 3 in reach A-B (17%). At the forested site, discharge during round 3 changed by 26% in reach A-B and 27% in reach B-C yet, these higher percentages represent extremely low volumetric changes (i.e., less than 1L/s). While discharge changed marginally during some injections, the relative nature of the SAS metrics (fraction of discharge labeled (f_{Qlabel}) and fraction of advective volume labeled (f_{VADV})) are not affected by these changes.

4. DISCUSSION

4.1 How Does Solute Transport Differ between Stream Sites?

The results showed the heavily impacted, agricultural site has a low capacity to store solutes within the reach while the relatively undisturbed, forested site has a high capacity with various mechanisms for storage. I recognize that solute transport processes may be different at longer timescales or greater spatial extent, and accordingly use the results of the field study to draw conclusion about storage available at the spatial and temporal scales reported in Table 1. Overall my results are in agreement with past studies that found transient storage had little influence over hydraulic transport in agricultural systems (Salehin *et al.*, 2003; Ensign and Doyle, 2005; Gooseff *et al.*, 2007) as well as, studies of forested headwater mountain streams within the Western United States that show the presence of hyporheic transient storage (Wondzell, 2006) and subsurface exchange (Covino and McGlynn, 2007; Payn *et al.*, 2009). Additionally, past studies (Harvey and Bencala, 1993; Cardenas *et al.*, 2004; Gooseff and Haggerty, 2005; Gooseff *et al.*, 2007) conclude that geomorphic complexity is an important driver of solute transport dynamics in streams. Therefore, to assist in the interpretation of the study results, I present a perceptual model (Figure 6) of each stream site to demonstrate how differences in channel geomorphology explain observed solute transport behavior.

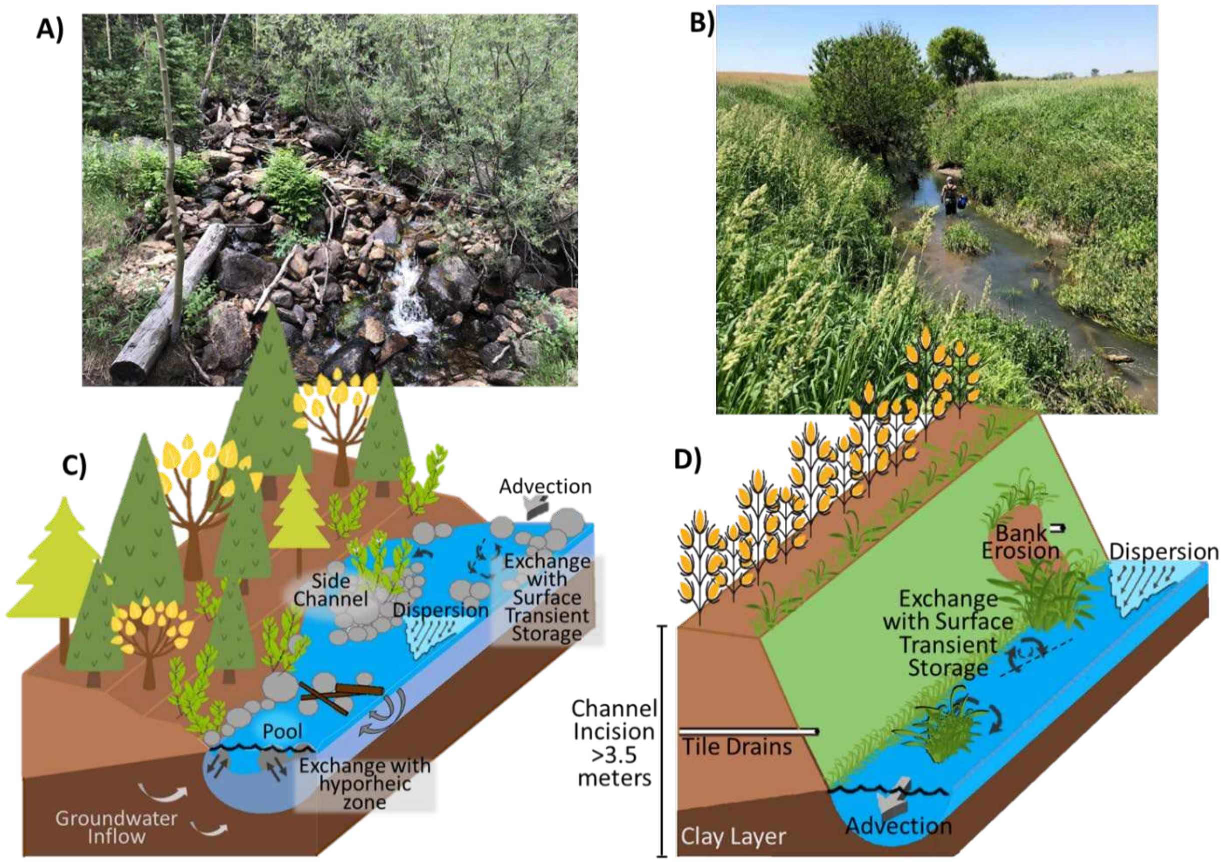

Figure 6: Field photos and perceptual model of each field site showing the characteristics of the study reaches. Perceptual model is annotated with factors affecting solute transport observed at each site. A, C) forested field site. B, D) agricultural site.

In the agricultural stream, I observed a lack of hyporheic and subsurface exchange indicated by the lack of gross loss to longer flowpaths, high fractions of the total in-stream discharge labeled with tracer (f_{Qlabel}), as well as the low fractions of the advective volume sampled (f_{VADV}). In combination, these observations suggest that tracer labeled water exchanged with small volumes of storage likely only within the channel. The agricultural stream is channelized and deeply incised into a silty clay loam substrate likely as a result of the impacts of agricultural land-use. Past studies (Bencala *et al.*, 1984; Harvey and Wagner, 2000; Tonina and Buffington, 2009; Angermann *et al.*, 2012; Stonedahl *et al.*, 2013; Zimmer and Lautz, 2014) have shown that presence of low conductivity streambed strata decrease hyporheic exchange. Additionally, hyporheic exchange is controlled by hydraulic gradients driven by channel slope, width, sinuosity and fluctuations in stage (Pinder and Sauer, 1971; Sharp, 1977; Larkin and Sharp Jr., 1992). The agricultural stream is characterized by a low-gradient (0.8% slope), straightened channel and little geomorphic heterogeneity (Figure 6), all of which limit hydraulic exchange. These factors combine to limit hyporheic and subsurface exchange restrict transient storage at the agricultural stream to in-channel zones with shorter residence times.

I conclude that the low magnitudes of *TSI*, γ, *CV* observed at the agricultural site compared to the forested site, are a result of the channelized form and planar, low-permeability silty clay loam bed. Observed f_{VADV} values close to one indicate the tracer labeled water likely did not experience any hyporheic exchange or subsurface storage again as a result of the geomorphic form and substrate of the agricultural stream. Riparian vegetation along the banks at the agricultural stream (Figure 6) enhances channel roughness which increases dispersion and surface transient storage (Ward *et al.*, 2013b). Additionally, the incision and channelization, discussed above, causes accelerated bank erosion and leads to banks with riparian vegetation sloughing into the channel (Figure 6). This mass failure of the stream banks forms bars within the channel and along the banks that split flow and adds variations in channel width that provides pockets of surface transient storage. Together the agricultural stream's incision into silty clay loam bed, channelization and limited geomorphic complexity create primarily surface transient storage and result in the low capacity to attenuate solutes.

In contrast, at the forested site, I observed both surface transient storage as well as hyporheic exchange and subsurface storage. The presence of surface transient storage was demonstrated through high median values of *TSI*, γ, and *CV*. Additionally, hyporheic exchange and subsurface storage was indicated by gross hydrologic losses and values of f_{VADV} much greater than 1. The forested site is a multi-thread channel with woody debris present and substrate ranging from small gravel to large cobbles and boulders (Figure 6). The heterogeneity within the stream channel provides a wide range of in-channel storage compartments including pools, side channels, and areas with backwater conditions and eddies. This channel complexity resulted in a broader range of observed *TSI* and mean arrival time values relative to the agricultural stream. Additionally, the forested stream channel is steep (21% slope) and contains both step-pool and cascade channel morphologies. Hyporheic transient storage is partially driven by hydraulic gradients and geomorphic complexity (Boano *et al.*, 2014; Wondzell and Gooseff, 2014) and surface transient storage can be enhanced by roughness elements such as woody debris, and channel complexities including variation in width, multi-thread channels, and meander bends(Ward *et al.*, 2013a). Overall, the channel roughness, and geomorphic heterogeneity provided a range of surface and subsurface transient storage mechanisms that promoted high solute attenuation in the forested stream.

4.2 How Does Solute Transport Vary at Changing Discharge Conditions?

I observed less variability in advective time scales and all associated transport metrics in the agricultural relative to the forested site. This may be due to the well-documented relationship between advective timescale and transient storage (Ward *et al.*, 2013a; Schmadel *et al.*, 2016). In the study design, I aimed to match the magnitude of advective timescales between sites by adjusting reach lengths. The goal of obtaining similar advective timescales in both the agricultural and forested streams was to enable cross-site comparison of solute transport processes. I was able to obtain similar orders of magnitude in advective timescales between the two study sites, but the forested stream had a broader range of advective travel times. Given that the tracer injections occurred at the lowest observed flows at the agricultural site (Figure 2D), there were not opportunities to evaluate longer advective timescales at this site. The narrow range of advective timescales at the agricultural site indicates a limited amount of variability in transport processes across the range of flows sampled. I infer that this low variation in transport processes is related to the agricultural streams homogenous channel structure (Figure 6). I see further evidence of limited transport processes in the narrow range in *TSI*, mean arrival time, γ, and *CV* observed at this site. In summary, the lack of broad changes in advective travel times suggests that transport mechanisms remain relatively constant across changing discharge conditions in the agricultural stream.

In the forested stream, I observed a broader distribution of advective travel times and associated transport metrics relative to the agricultural stream. The greater variation in transport metrics is likely a result of the geomorphic heterogeneity in the forested stream and changing flowpaths across varying discharge. For example, at longer advective timescales (i.e., lower discharge) I observed an increase in gross loss indicating movement of water from the surface into subsurface flowpaths. This is further demonstrated by the high values of f_{VADV} at longer advective travel times that indicate tracer labeled water experienced a large volume of storage and exchanged with subsurface storage zones. I observed decreasing holdback values at longer advective travel times which indicates that solutes were retained less within the system. I hypothesize that at short advective times (or high discharge conditions) the stream water labeled with tracer exchanged with a variety of available surface transient storage zones (e.g., large pools and side channels) and thus was delayed in the downstream transport, however, as advective times increased (discharge decreased) less types of surface transient storage were available for stream water exchange (e.g., pools decreased in size and side channels became disconnected). Yet, less types of storage in this system does not result in a lack of solute retention but rather a change in mechanism. At longer advective times, solutes move through available storage compartments (surface transient storage in dead zones along the side of the channel and hyporheic storage) more slowly and thus the forested stream continues to have a high capacity for solute retention. I observed this continued high capacity through the increased values of *TSI* at longer advective times. As streamflow recedes to baseflow conditions there are associated changes in turbulent energy, wetted geometry, and hydraulic gradients (Leopold and Maddock, 1953) that can activate or deactivate different solute transport mechanisms in geomorphically complex and heterogeneous stream channels.

5. CONCLUSION

I evaluated net changes in discharge, gross hydrologic loss, temporal moments, and SAS functions to interpret solute transport behavior in a high-gradient forested stream and a heavily modified, low-gradient, agricultural stream. By combining these analyses I was able to infer differences in transient storage mechanisms (i.e., surface or subsurface) between the stream sites and across varying discharge conditions. The distinction between surface and subsurface transient storage is important because subsurface storage is more likely to result in long residence times and has the potential to attenuate downstream solute fluxes more strongly that in-channel storage. The SAS approach implemented in my study quantifies the volume of storage that is actively turning over which indicates whether tracer exchanged with only small volumes of surface storage or larger volumes of both surface and hyporheic transient storage.

This study builds on past studies (Harvey and Bencala, 1993; Cardenas *et al.*, 2004; Gooseff and Haggerty, 2005; Gooseff *et al.*, 2007) that identify geomorphic complexity to be an important driver of solute transport dynamics in streams. I further quantify how streams with contrasting morphologies exhibit different solute transport behavior and investigated how these factors vary through changes in discharge conditions. In a geomorphically complex, relatively undisturbed, forested stream there was a broad range of transport behavior and evidence of substantial exchange with both surface and hyporheic transient storage. In this stream system, changing discharge conditions activated or deactivated different solute transport mechanisms and greatly impacted advective travel time. Results from this forested stream demonstrate how geomorphic complexity within a natural system can promote heterogeneity in solute transport processes that effectively retain solutes and attenuate downstream fluxes over timescales ranging from minutes to days.

Conversely, in a simplified, agricultural stream there was a narrow range of solute transport behavior and only exchange between the advective main channel and surface transient storage. The lack of geomorphic heterogeneity in the agricultural stream resulted in similar solute transport mechanisms across varying discharge conditions and therefore limited the variability in advective travel times. Results from the agricultural stream highlight how the impacts of land use can have compounding effects. Agricultural land use typically increases nutrient loads (e.g., Nitrogen and Phosphorus) to streams through fertilizer application (Pierce *et al.*, 2012). Simultaneously, hydrologic alteration including increased connection to the terrestrial landscapes via tile drains and channelization that disconnects streams from their floodplains can cause increased discharge and decreased biogeochemical processing (Pierce *et al.*, 2012). This results in a modified stream system with increased loading and inhibited transient storage mechanisms which can combine to have deleterious effects for downstream water quality. Future studies, should work to quantify how these inhibited storage mechanisms resulting from land use change and channel simplification impact biogeochemical processes to manage and mitigate impacts of land use on lotic system function.

REFERENCES

Ader E, Wohl E, McFadden S, Singha K. 2021. Logjams as a driver of transient storage in a mountain stream. *Earth Surface Processes and Landforms* **46** (3): 701–711 DOI: 10.1002/esp.5057

Angermann L, Krause S, Lewandowski J. 2012. Application of heat pulse injections for investigating shallow hyporheic flow in a lowland river. *Water Resources Research* **48** (10): 1–16 DOI: 10.1029/2012WR012564

Bencala KE, Walters RA. 1983. Simulation of solute transport in a mountain pool-and-riffle stream: A transient storage model. *Water Resources Research* **19** (3): 718–724 DOI: 10.1029/WR019i003p00718

Bencala KE, Kennedy VC, Zellweger GW, Jackman AP. 1984. An Experimental Analysis of Cation and Anion Transport. *Water Resources* **20** (12): 1797–1803

Boano F, Harvey JW, Marion A, Packman AI, Revelli R, Ridolfi L, Wörman A. 2014. Hyporheic flow and transport processes: Mechanisms, models, and biogeochemical implications. *Reviews of Geophysics* **52** (4): 603–679 DOI: 10.1002/2012RG000417

Briggs MA, Gooseff MN, Arp CD, Baker MA. 2009. A method for estimating surface transient storage parameters for streams with concurrent hyporheic storage. *Water Resources Research* **45** (February): 1–13 DOI: 10.1029/2008WR006959

Brunke M, Gonser T. 1997. The ecological significance of exchange processes between rivers and groundwater. *Freshwater Biology* **37** (1): 1–33 DOI: 10.1046/j.1365-2427.1997.00143.x

Butturini A, Sabater F. 1999. Importance of transient storage zones for ammonium and phosphate retention in a sandy-bottom Mediterranean stream. *Freshwater Biology* **41** (3): 593–603 DOI: 10.1046/j.1365-2427.1999.00406.x

Cardenas MB, Wilson JL, Zlotnik VA. 2004. Impact of heterogeneity, bed forms, and stream curvature on subchannel hyporheic exchange. *Water Resources Research* **40** (8): 8307 DOI: 10.1029/2004WR003008

Covino T. 2017. Hydrologic connectivity as a framework for understanding biogeochemical flux through watersheds and along fluvial networks. *Geomorphology* **277**: 133–144 DOI: 10.1016/j.geomorph.2016.09.030

Covino TP, McGlynn BL. 2007. Stream gains and losses across a mountain-to-valley transition: Impacts on watershed hydrology and stream water chemistry. *Water Resources Research* **43** (10) DOI: 10.1029/2006WR005544

Danckwerts P V. 1953. Continuous flow systems. Distribution of residence times. *Chemical Engineering Science* **2** (1): 1–13 DOI: 10.1016/0009-2509(53)80001-1

David MB, Stephen AE, Grosso J Del, Xuetao AE, Ae H, Marshall EP, Gregory AE, Mcisaac F, William AE, Parton J, et al. 2009. Modeling denitrification in a tile-drained, corn and soybean agroecosystem of Illinois, USA. *Biogeochemistry* **93**: 7–30 DOI: 10.1007/s10533-008-9273-9

DeWalle DR, Swistock BR, Johnson TE, McGuire KJ. 2000. Potential effects of climate change and urbanization on mean annual streamflow in the United States. *Water Resources Research* **36** (9): 2655–2664 DOI: 10.1029/2000WR900134

Drummond JD, Covino TP, Aubeneau AF, Leong D, Patil S, Schumer R, Packman AI. 2012. Effects of solute breakthrough curve tail truncation on residence time estimates: A synthesis of solute tracer injection studies. *Journal of Geophysical Research: Biogeosciences* **117** (3): 1–11 DOI: 10.1029/2012JG002019

Ensign SH, Doyle MW. 2005. In-channel transient storage and associated nutrient retention: Evidence from experimental manipulations. *Limnology and Oceanography* **50** (6): 1740–1751 DOI: 10.4319/lo.2005.50.6.1740

Fabian MW, Endreny TA, Bottacin-Busolin A, Lautz LK. 2011. Seasonal variation in cascade-driven hyporheic exchange, northern Honduras. *Hydrological Processes* **25** (10): 1630–1646 DOI: 10.1002/hyp.7924

Fischer HB, List JE, Koh R, Imberger J. 1979. *Mixing in inland and coastal waters.* Academic: San Diego, CA.

Ghisalberti M. 2002. Mixing layers and coherent structures in vegetated aquatic flows. *Journal of Geophysical Research* **107** (C2) DOI: 10.1029/2001jc000871

Gibson D. 2018. How is it possible to convert conductivity of NaCl solution (in uS) to its salinity (NaCl concentration, in ppm)?

Gooseff MN, Haggerty R. 2005. A modelling study of hyporheic exchange pattern and the sequence, size, and spacing of stream bedforms in mountain stream networks, Oregon, USA. *Process* **19**: 2915–2929 DOI: 10.1002/hyp.5790

Gooseff MN, Hall RO, Tank JL. 2007. Relating transient storage to channel complexity in streams of varying land use in Jackson Hole, Wyoming. *Water Resources Research* **43** (1): 1–10 DOI: 10.1029/2005WR004626

Gupta A, Cvetkovic V. 2000. Temporal moment analysis of tracer discharge in streams: Combined effect of physicochemical mass transfer and morphology. *Water Resources Research* **36** (10): 2985–2997 DOI: 10.1029/2000WR900190

Harman CJ, Ward AS, Ball A. 2016. How does reach-scale stream-hyporheic transport vary with discharge? Insights from rSAS analysis of sequential tracer injections in a headwater mountain stream. *Water Resources Research* **52** (9): 7130–7150 DOI: 10.1002/2016WR018832

Harvey JW, Bencala KE. 1993. The Effect of streambed topography on surface-subsurface water exchange in mountain catchments. *Water Resources Research* **29** (1): 89–98 DOI: 10.1029/92WR01960

Harvey JW, Wagner BJ. 2000. Quantifying hydrologic interactions between streams and their subsurface hyporheic zones. In *Streams and Ground Waters*, Jones JB, , Mulholland PJ (eds).Academic Press: San Diego, CA; 3–44. DOI: 10.1016/B978-012389845-6/50002-8

Harvey JW, Wagner BJ, Bencala KE. 1996. Evaluating the reliability of the stream tracer approach to characterize stream-subsurface water exchange. *Water Resources Research* **32** (8): 2441–2451 DOI: 10.1029/96WR01268

Jackson TR, Apte S V, Haggerty R, Budwig R. 2015. Flow structure and mean residence times of lateral cavities in open channel flows: influence of bed roughness and shape. *Environmental Fluid Mechanics* **15** (5): 1069–1100 DOI: 10.1007/s10652-015-9407-2

Johnson ZC, Warwick JJ, Schumer R. 2014. Factors affecting hyporheic and surface transient storage in a western U.S. river. *Journal of Hydrology* **510**: 325–339 DOI: 10.1016/j.jhydrol.2013.12.037

Jones JA, Swanson FJ, Wemple BC, Snyder KU. 2000. Effects of Roads on Hydrology, Geomorphology, and Disturbance Patches in Stream Networks. *Conservation Biology* **14** (1): 76–85 DOI: 10.1046/j.1523-1739.2000.99083.x

Kilpatrick FA, Cobb ED. 1985. Measurement of discharge using tracers DOI: 10.3133/twri03A16

Kondolf GM, Boulton AJ, O'daniel S, Poole GC, Rahel FJ, Stanley EH, Wohl E, Bång A, Carlstrom J, Cristoni C, et al. 2006. Process-Based Ecological River Restoration: Visualizing Three-Dimensional Connectivity and Dynamic Vectors to Recover Lost Linkages. *Ecology and Society* **11** (2)

Krause S, Hannah DM, Fleckenstein JH, Heppell CM, Kaeser D, Pickup R, Pinay G, Robertson AL, Wood PJ. 2011. Inter-disciplinary perspectives on processes in the hyporheic zone. *Ecohydrology* **4** (4): 481–499 DOI: 10.1002/eco.176

Larkin RG, Sharp Jr. JM. 1992. On the relationship between river-basin geomorphology, aquifer hydraulics, and ground-water flow direction in alluvial aquifers. *GSA Bulletin* **104** (12): 1608–1620 DOI: 10.1130/0016-7606(1992)104<1608:OTRBRB>2.3.CO;2

Leopold LB, Maddock T. 1953. The Hydraulic Geometry of Stream Channels and Some Physiographic Implications. Washington, D.C.

Magliozzi C, Grabowski R, Packman A, Krause S. 2017. Scaling down hyporheic exchange flows: from catchments to reaches. *Hydrology and Earth System Sciences Discussions*: 1–53 DOI: 10.5194/hess-2016-683

Mason SJK, McGlynn BL, Poole GC. 2012. Hydrologic response to channel reconfiguration on Silver Bow Creek, Montana. *Journal of Hydrology* **438**–**439**: 125–136 DOI: 10.1016/j.jhydrol.2012.03.010

McIsaac GF, Hu X. 2004. Net N input and riverine N export from Illinois agricultural watersheds with and without extensive tile drainage. *Biogeochemistry* **70** (2): 251–271 DOI: 10.1023/B:BIOG.0000049342.08183.90

Morrice JA, Valett HM, Dahm CN, Campana ME. 1997. Alluvial Characteristics, Groundwater–Surface Water Exchange and Hydrological Retention in Headwater Streams. *Hydrological Processes* **11** (3): 253–267 DOI: 10.1002/(SICI)1099-1085(19970315)11:3<253::AID-HYP439>3.0.CO;2-J

Natural Resources Conservation Service. Web Soil Survey. *United States Department of Agriculture* Available at: https://websoilsurvey.nrcs.usda.gov/app/WebSoilSurvey.aspx [Accessed 6 July 2021]

Payn RA, Gooseff MN, McGlynn BL, Bencala KE, Wondzell SM. 2009. Channel water balance and exchange with subsurface flow along a mountain headwater stream in Montana, United States. *Water Resources Research* **45** (11) DOI: 10.1029/2008WR007644

Pierce SC, Kröger R, Pezeshki R. 2012. Managing artificially drained low-gradient agricultural headwaters for enhanced ecosystem functions. *Biology* **1** (3): 794–856 DOI: 10.3390/biology1030794

Pinder GF, Sauer SP. 1971. Numerical Simulation of Flood Wave Modification Due to Bank Storage

Effects. *Water Resources Research* **7** (1): 63–70 DOI: 10.1029/WR007i001p00063

Ries III KG, Newson JK, Smith MJ, Guthrie JD, Steeves PA, Haluska T, Kolb KR, Thompson RF, Santoro RD, Vraga HW. 2017. StreamStats, version 4. Reston, VA. DOI: 10.3133/fs20173046

Runkel RL, McKnight DM, Rajaram H. 2003. Modeling hyporheic zone processes. *Advances in Water Resources* **26** (9): 901–905 DOI: 10.1016/S0309-1708(03)00079-4

Salehin M, Packman AI, Wörman A. 2003. Comparison of transient storage in vegetated and unvegetated reaches of a small agricultural stream in Sweden: Seasonal variation and anthropogenic manipulation. *Advances in Water Resources* **26** (9): 951–964 DOI: 10.1016/S0309-1708(03)00084-8

Schmadel NM, Neilson BT, Stevens DK. 2010. Approaches to estimate uncertainty in longitudinal channel water balances. *Journal of Hydrology* **394** (3–4): 357–369 DOI: 10.1016/j.jhydrol.2010.09.011

Schmadel NM, Ward AS, Kurz MJ, Fleckenstein JH, Zarnetske JP, Hannah DM, Blume T, Vieweg M, Blaen PJ, Schmidt C, et al. 2016. Stream solute tracer timescales changing with discharge and reach length confound process interpretation. *Water Resources Research* **52** (4): 3227–3245 DOI: 10.1002/2015WR018062

Schmid BH, Innocenti I, Sanfilippo U. 2010. Characterizing solute transport with transient storage across a range of flow rates: The evidence of repeated tracer experiments in Austrian and Italian streams. *Advances in Water Resources* **33** (11): 1340–1346 DOI: 10.1016/j.advwatres.2010.06.001

Sharp JM. 1977. Limitations of Bank-Storage Model Assumptions. *Journal of Hydrology* **35**: 31–47

Stanford JA, Ward J V. 1988. The hyporheic habitat of river ecosystems. *Nature* **335** (6185): 64–66 DOI: 10.1038/335064a0

Stonedahl SH, Harvey JW, Packman AI. 2013. Interactions between hyporheic flow produced by stream meanders, bars, and dunes. *Water Resources Research* **49** (9): 5450–5461 DOI: 10.1002/wrcr.20400

Thomas SA, Maurice Valett H, Webster JR, Mulholland PJ. 2003. A regression approach to estimating reactive solute uptake in advective and transient storage zones of stream ecosystems. *Advances in Water Resources* **26** (9): 965–976 DOI: 10.1016/S0309-1708(03)00083-6

Tonina D, Buffington JM. 2009. Hyporheic exchange in mountain rivers I: Mechanics and environmental effects. *Geography Compass* **3** (3): 1063–1086 DOI: 10.1111/j.1749-8198.2009.00226.x

U.S. Environmental Protection Agency. 2020. National Rivers and Streams Assessment 2013-2014: A Collaborative Survey. EPA 841-R-19-001. Washington, DC. Available at: http://www.epa.gov/national-aquatic-resource-surveys/data-national-aquatic-resource-surveys. [Accessed 7 April 2021]

Walter RC, Merritts DJ. 2008. Natural streams and the legacy of water-powered mills. *Science* **319** (5861): 299–304 DOI: 10.1126/science.1151716

Ward AS. 2016. The evolution and state of interdisciplinary hyporheic research. *Wiley Interdisciplinary Reviews: Water* **3** (1): 83–103 DOI: 10.1002/wat2.1120

Ward AS, Gooseff MN, Singha K. 2013a. How Does Subsurface Characterization Affect Simulations of Hyporheic Exchange? *Ground Water* **51** (1): 14–28 DOI: 10.1111/j.1745-6584.2012.00911.x

Ward AS, Gooseff MN, Voltz TJ, Fitzgerald M, Singha K, Zarnetske JP. 2013b. How does rapidly changing discharge during storm events affect transient storage and channel water balance in a headwater mountain stream? *Water Resources Research* **49** (9): 5473–5486 DOI: 10.1002/wrcr.20434

Ward AS, Kurz MJ, Schmadel NM, Knapp JLA, Blaen PJ, Harman CJ, Drummond JD, Hannah DM, Krause S, Li A, et al. 2019a. Solute transport and transformation in an intermittent, headwater mountain stream with diurnal discharge fluctuations. *Water (Switzerland)* **11** (11) DOI: 10.3390/w11112208

Ward AS, Morgan JA, White JR, Royer T V. 2018. Streambed restoration to remove fine sediment alters reach-scale transient storage in a low-gradient fifth-order river, Indiana, USA. *Hydrological Processes* **32** (12): 1786–1800 DOI: 10.1002/hyp.11518

Ward AS, Payn RA, Gooseff MN, McGlynn BL, Bencala KE, Kelleher CA, Wondzell SM, Wagener T. 2013c. Variations in surface water-ground water interactions along a headwater mountain stream: Comparisons between transient storage and water balance analyses. *Water Resources Research* **49** (6): 3359–3374 DOI: 10.1002/wrcr.20148

Ward AS, Wondzell SM, Schmadel NM, Herzog S, Zarnetske JP, Baranov V, Blaen PJ, Brekenfeld N, Chu R, Derelle R, et al. 2019b. Spatial and temporal variation in river corridor exchange across a 5{th}-order mountain stream network. *Hydrology and Earth System Sciences* **23** (12): 5199–5225 DOI: 10.5194/hess-23-5199-2019

Wondzell SM. 2006. Effect of morphology and discharge on hyporheic exchange flows in two small streams in the Cascade Mountains of Oregon, USA. *Hydrological Processes* **20** (2): 267–287 DOI: 10.1002/hyp.5902

Wondzell SM, Gooseff MN. 2014. Geomorphic Controls on Hyporheic Exchange Across Scales: Watersheds to Particles. *Treatise in Fluvial Geomorpholgy* **9**

Zarnetske JP, Gooseff MN, Brosten TR, Bradford JH, McNamara JP, Bowden WB. 2007. Transient storage as a function of geomorphology, discharge, and permafrost active layer conditions in Arctic tundra streams. *Water Resources Research* **43** (7): 7410 DOI: 10.1029/2005WR004816

Zellweger GW, Avanzino RJ, Bencala KE, Peck DL. 1989. Comparison of tracer-dilution and current-meter discharge measurements in a small gravel-bed stream, Little Lost Man Creek, California DOI: 10.3133/wri894150

Zimmer MA, Lautz LK. 2014. Temporal and spatial response of hyporheic zone geochemistry to a storm event. *Hydrological Processes* **28** (4): 2324–2337 DOI: 10.1002/hyp.9778

APPENDIX A: SUMMARY OF VARIABLE USED IN ANALYSIS

Channel Water Balance

$C(t) = \ background\ corrected\ NaCl\ concentration\ [gL^{-1}]$

$Q_D = discharge\ at\ downstream\ monitoring\ \ site[Ls^{-1}]$

$Q_U = discharge\ at\ upstream\ monitoring\ site\ [Ls^{-1}]$

$Qnet\% = change\ in\ discharge, negative\ value\ indicates\ lossing\ reach,$

$postive\ indicates\ gaining\ reach\ [\%]$

$C_{UD} = observed\ tracer\ concentration\ at\ downstream\ monitoring\ site$

$from\ upstream\ tracer\ release\ [gL^{-1}]$

$M_R = tracer\ mass\ recovered\ [g]$

$M_U = tracer\ mass\ injected\ at\ upstream\ site\ [g]$

$M_L = tracer\ mass\ loss\ [g]$

$\%\ Gross\ Loss = percent\ gross\ loss\ [\%]$

Temporal Moment Analysis

$t = time\ since\ injection\ [\mathrm{min}]$

$TSI = transient\ storage\ index\ [min]$

$c(t) = \ normalized\ background\ corrected\ NaCl\ concentration$

$M_1 = first\ temporal\ moment,\ \ mean\ arrival\ time\ [min]$

$\mu_n = nth - order\ central\ temporal\ moment\ [min^n]$

$CV = coefficient\ of\ variation$

$\gamma = Skewness$

$H = Holdback$

$F(t) = variable\ of\ integration\ used\ in\ calculation\ of\ holdback$

StorAge Selection Function (SAS)

$p_Q(T) = probability\ density\ of\ the\ (forward)\ transit\ time\ distribution$

$P_Q(T)$
$= \textit{Cumulative form of the probability density of the (forward) transit time distribution}$

$Q_T(T) = \textit{Age} - \textit{ranked discharge}\ [Ls^{-1}]$

$S_T(T) = \textit{Age} - \textit{ranked storage}\ [L]$

$Q_{comp} = \textit{Complement to the age} - \textit{ranked discharge}\ [Ls^{-1}]$

$S_{comp}(T) = \textit{Complement to the age} - \textit{ranked storage}\ [L]$

$S_{ref} = \mathrm{S}_{T,max} = \textit{Maximum volume of storage that is actively turning over on timescales of our experiement}\ [L]$

$f_{Qlabel}(T) = \textit{Fraction of the in} - \textit{stream discharge labeled by tracer}$

$f_{VADV}(T) = \textit{Fraction of the advective volume sampled labeled by tracer}$

$V_{adv} = \textit{Volume of stream water in advection}\ [L]$